International Journal of Heat and Mass Transfer 68 (2014) 299–309

Contents lists available at ScienceDirect

International Journal of Heat and Mass Transfer

journal homepage: www.elsevier.com/locate/ijhmt

# Heat transfer enhancement by layering of two immiscible co-flows

A.-R.A. Khaled [a], K. Vafai [b,*]

[a] King Abdulaziz University, Mechanical Engineering Department, Jeddah 21589, Saudi Arabia
[b] University of California at Riverside, Mechanical Engineering Department, Riverside, CA 92521, USA

ARTICLE INFO

*Article history:*
Received 31 August 2013
Received in revised form 17 September 2013
Accepted 17 September 2013

*Keywords:*
Heat transfer
Enhancement
Immiscible fluids
Minichannel
Convection

ABSTRACT

Enhancement of heat transfer in minichannels due to co-flowing of two immiscible fluids in a direct contact is investigated in this work. Different fluid combinations are analyzed. The momentum and energy equations for both flows are solved analytically and numerically. The numerical and analytical solutions are found to be in good agreement. A parametric study including the influence of fluids relative viscosity, thermal conductivity, thermal capacity and height ratios is conducted for various Peclet numbers. Different ranges of the parameters that augment the heat transfer are obtained, and different physical aspects of the problem are discussed. For practical fluid combinations with small Peclet numbers, the enhancement factor can increase up to 2.6 folds. However, that increase is about 1.2 folds when the Peclet number is increased by two orders of magnitude. This work establishes the mechanisms for heat transfer enhancement utilizing two immiscible co-flows.



## 1. Introduction

A review of recent heat transfer literature [1–3] reveals that large number of investigations was devoted to the topic of heat transfer enhancement. Most of these works considered at least one of the following enhancement mechanisms: (a) stream profiling [4,5] such as using twisted tapes, spirals, and wire coils, (b) fins such as slotted and louvered fins [6,7], (c) electrohydrodynamic effects [8], (d) surface coatings [9], (e) additives [10,11], (f) acoustic streaming [2], (g) turbulators [2] and, (h) flow and velocity amplifications [12–14]. Additional reviews in this area have shown an increased interest in enhancement technology [15,16]. A number of these works introduce new concepts in this area [17–22].

Heat transfer Enhancement utilizing an immiscible fluid co-flowing with the coolant flow in a direct contact manner has not received much attention by researchers [1–3,15,16,22]. As such, this subject is considered as the main topic of the present work. Immiscible fluids having smaller viscosity or larger specific heat than the coolant can enhance the heat transfer. This is because they can enhance the velocity near the heated plate, widening the thermal entry region or amplifying the coolant flow rate. These effects are the major causes for heat transfer enhancement by laminar flows. Therefore, the present work is additionally aimed to specify ranges for thermophysical properties and flow conditions that can result heat transfer enhancement by co-flowing two immiscible fluids.

One of the main advantages of heat transfer enhancement by co-flowing of two immiscible fluids in direct contact manner is that both flows are subject to the same pressure gradient. In contrast, the pressure gradient of the counter-flowing system decrease to zero then changes sign and starts to decrease below zero. As a result, the fluid flow rates in the co-flowing system are expected to be larger than those in the counter-flowing system. Moreover, for short channels with co-flowing system, the secondary fluid temperatures at the inlet of the primary flow are much smaller than those of the counter-flowing system. This effect elevates the convection heat transfer coefficient between the heated boundary and the adjacent primary flow due to thermal entry region. Finally, as the micro-channel geometry may cause inadequate operation of efficient enhancement methods [23–25], co-flowing of two immiscible fluids can become an attractive alternative.

In the present work, heat transfer through two layered immiscible fluid flow within a horizontal minichannel is analyzed. For all analyzed cases, the density and the thermal conductivity of the primary fluid residing on the heated boundary are considered to be larger than those of the other fluid, referred to as the secondary fluid. The dynamic viscosity and the volumetric thermal capacity of the secondary fluid are allowed to be either larger or smaller than those of the primary fluid. Both momentum and energy transport equations are solved for each flow using analytical and numerical methods. Various analytical solutions for the temperature field under applicable constraints are obtained and validated against the numerical solution. A parametric study of the heat transfer enhancement is made to identify ranges of controlling parameters that reveal favorable enhancement attributes.

* Corresponding author. Tel.: +1 951 827 2135; fax: +1 951 827 2899.
*E-mail address:* vafai@engr.ucr.edu (K. Vafai).

0017-9310/$ - see front matter © 2013 Elsevier Ltd. All rights reserved.
http://dx.doi.org/10.1016/j.ijheatmasstransfer.2013.09.040

**Nomenclature**

| | |
|---|---|
| $a$ | channel aspect ratio (a = H/$L$) |
| $a_1$, $a_2$ | (primary, secondary) flow aspect ratio ($a_1 = \delta/L,\ a_2 = [H-\delta]/L$) |
| $C_1$, $C_2$ | (primary, secondary) flow thermal capacity (W K$^{-1}$) |
| $c_{p1}$, $c_{p2}$ | (primary, secondary) fluid specific heat (J kg$^{-1}$ K$^{-1}$) |
| $H$ | channel height (m) |
| $h_1$ | convection coefficient at the hot boundary (W m$^{-2}$ K$^{-1}$) |
| $h_I$ | convection coefficient between interface and secondary flow (W m$^{-2}$ K$^{-1}$) |
| $k_1$, $k_2$ | (primary, secondary) fluid thermal conductivity (W m$^{-1}$ K$^{-1}$) |
| $L$ | channel length (m) |
| $\dot{m}_1, \dot{m}_2$ | (primary, secondary) fluid mass flow rate (kg s$^{-1}$) |
| $Nu_1$ | Nusselt number between hot boundary and primary flow ($Nu_1 = h_1\delta/k_1$) |
| $Nu_2$ | Nusselt number between interface and secondary flow, Eq. (20) |
| $P_1$, $P_2$ | (primary, secondary) flow ideal pumping power (W) |
| $P_t$ | total ideal pumping power (W) |
| $p_1$, $p_2$ | (primary, secondary) fluid pressure (kg m$^{-1}$ s$^{-2}$) |
| $\overline{p}_1, \overline{p}_2$ | (primary, secondary) fluid dimensionless pressure, Eqs. 4(h, i) |
| $Pe_1$, $Pe_2$ | (primary, secondary) flow Peclet number ($Pe_{1,2} = Re_{1,2}Pr_{1,2}$) |
| $Pr_1$, $Pr_2$ | (primary, secondary) fluid Prandtl number ($Pr_{1,2} = \mu_{1,2}(c_p)_{1,2}/k_{1,2}$) |
| $q''_s$ | heat flux at hot boundary (W m$^{-2}$) |
| $q''_I$ | heat flux at interface (W m$^{-2}$) |
| $Re_1$, $Re_2$ | (primary, secondary) flow Reynolds number, Eqs. 5(d, e) |
| $T_1$, $T_2$ | (primary, secondary) fluid temperature (K) |
| $u_1$, $u_2$ | (primary, secondary) fluid axial velocity (m s$^{-1}$) |
| $\overline{u}_1, \overline{u}_2$ | (primary, secondary) fluid dimensionless velocity ($\overline{u}_{1,2} = u_{1,2}/u_{(1,2)avg}$) |
| $v_1$, $v_2$ | (primary, secondary) fluid transverse velocity (m s$^{-1}$) |
| $\overline{v}_1, \overline{v}_2$ | dimensionless ($v_1, v_2$) transverse velocity ($\overline{v}_{1,2} = v_{1,2}/[(\delta/L)u_{(1,2)avg}]$) |
| $x, \overline{x}$ | (dimensional, dimensionless) axial distance ((m), $\overline{x} = x/L$) |
| $y_1$, $y_2$ | normal (primary, secondary) system coordinate (m) |
| $\overline{y}_1, \overline{y}_2$ | dimensionless ($y_1$,$y_2$) coordinate ($\overline{y}_1 = y_1/\delta,\ \ \overline{y}_2 = y_2/[H-\delta]$) |
| *Greek symbols* $\gamma$ | second thermal performance factor, Eq. (23) |
| $\lambda$ | heat transfer enhancement factor, Eq. (22) |
| $\mu_1$, $\mu_2$ | (primary, secondary) fluid dynamic viscosity (kg m$^{-1}$ s$^{-1}$) |
| $\theta_1$, $\theta_2$ | dimensionless (primary, secondary) fluid temperature, Eqs. 4(j, k) |
| $\rho_1$, $\rho_2$ | (primary, secondary) fluid density (kg m$^{-3}$) |
| *Subscripts* | |
| *avg* | average quantity |
| *I* | quantity at interface |
| *i* | quantity at inlet |
| *o* | quantity at outlet |
| *m* | mean bulk value of the quantity |
| *r* | quantity when primary flow occupying the channel height |
| *W* | quantity at the hot boundary |

## 2. Problem formulation

### 2.1. Generalized two-dimensional model

Consider a two-dimensional horizontal minichannel of height $H$ which is much smaller than its length $L$. Consider two immiscible fluids co-flowing inside the minichannel. The primary fluid has specific heat $c_{p1}$, thermal conductivity $k_1$, dynamic viscosity $\mu_1$ and density $\rho_1$. The corresponding properties of the secondary fluid are $c_{p2}$, $k_2$, $\mu_2$ and $\rho_2$. The primary fluid is considered to be denser than the secondary fluid ($\rho_1 > \rho_2$) so it will line up against the lower boundary. This boundary is considered to be heated with a constant heat flux $q''_s$. The upper boundary of the minichannel is considered to be adiabatic so that both co-flows advect the total heat transfer from the source. In addition, the secondary fluid is considered to flow between the upper boundary of the minichannel and the upper boundary of the primary fluid flow in a co-current direction as shown in Fig. 1. The resulting system has a perfect direct contact interface between the fluids. This results in the maximum heat transfer enhancement ratio.

The height of the primary fluid flow is $\delta$ while that of the secondary fluid flow is $H-\delta$. Both fluids have the same inlet pressure $p_i$ and the same exit pressure $p_o$. The $x$-axis is taken along the minichannel starting from its inlet as shown in Fig. 1. The $y_1$-axis is taken along the minichannel transverse direction starting from its lower boundary. The $y_2$-axis is taken along the minichannel transverse direction starting from the upper boundary of the primary fluid flow at $y_1 = \delta$ as shown in Fig. 1. The momentum and energy equations for internal flows are applicable to the present problem [26,27]. These equations for both fluids have the following dimensionless forms:

$$\frac{\partial \overline{u}_{1,2}}{\partial \overline{x}} + \frac{\partial \overline{v}_{1,2}}{\partial \overline{y}_{1,2}} = 0 \tag{1a, 1b}$$

$$a_{1,2}Re_{1,2}\left[\overline{u}_{1,2}\frac{\partial \overline{u}_{1,2}}{\partial \overline{x}} + \overline{v}_{1,2}\frac{\partial \overline{u}_{1,2}}{\partial \overline{y}_{1,2}}\right] = -12\frac{d\overline{p}_{1,2}}{d\overline{x}} + (a_{1,2})^2\frac{\partial^2 \overline{u}_{1,2}}{\partial \overline{x}^2} + \frac{\partial^2 \overline{u}_{1,2}}{\partial \overline{y}_{1,2}^2} \tag{2a, 2b}$$

$$a_{1,2}Re_{1,2}Pr_{1,2}\left[\overline{u}_{1,2}\frac{\partial \theta_{1,2}}{\partial \overline{x}} + \overline{v}_{1,2}\frac{\partial \theta_{1,2}}{\partial \overline{y}_{1,2}}\right] = (a_{1,2})^2\frac{\partial^2 \theta_{1,2}}{\partial \overline{x}^2} + \frac{\partial^2 \theta_{1,2}}{\partial \overline{y}_{1,2}^2} \tag{3a, 3b}$$

where

$$\overline{x} = \frac{x}{L};\quad \overline{y}_1 = \frac{y_1}{\delta};\quad \overline{y}_2 = \frac{y_2}{H-\delta}; \tag{4a-c}$$

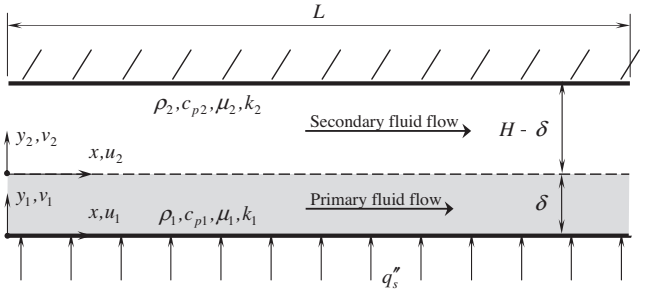


**Fig. 1.** Schematic diagram the coordinates system for the two dimensional channel with two co-flows of immiscible fluids.

$$\overline{u}_1(\overline{x},\overline{y}_1)=\frac{u_1(x,y_1)}{u_{1avg}};\quad \overline{u}_2(\overline{x},\overline{y}_2)=\frac{u_2(x,y_2)}{u_{2avg}};$$
$$\overline{v}_1(\overline{x},\overline{y}_1)=\frac{v_1(x,y_1)}{(\delta/L)u_{1avg}};\quad \overline{v}_2(\overline{x},\overline{y}_2)=\frac{v_2(x,y_2)}{([H-\delta]/L)u_{2avg}};\qquad (4d\text{-}i)$$
$$\overline{p}_1(\overline{x})=\frac{p(x)-p_o}{12L\mu_1u_{1avg}/\delta^2};\quad \overline{p}_2(\overline{x})=\frac{p(x)-p_o}{12L\mu_2u_{2avg}/(H-\delta)^2}$$

$$\theta_1(\overline{x},\overline{y}_1)=\frac{T_1(x,y_2)-T_i}{q_s''\delta/k_1};\quad \theta_2(\overline{x},\overline{y}_2)=\frac{T_2(x,y_2)-T_i}{q_s''(H-\delta)/k_2};\qquad (4j,4k)$$

$u_1$ and $u_2$ are the primary and secondary flow velocity components along the $x$-direction, respectively. Their mean values are given as $u_{1avg}$ and $u_{2avg}$ and $v_1$ and $v_2$ are the primary and secondary flows velocity components along the $y_1$ and $y_2$ directions and $Pr_1$ and $Pr_2$ are the Prandtl numbers of the primary and secondary fluids, respectively. The scaling quantities used in Eqs. 4(a-k) are recommended so that the thermal entrance effects can be studied [28]. The dimensionless parameters $a_1$, $a_2$, $Re_1$ and $Re_2$ are given by:

$$a_1=a\left(\frac{\delta}{H}\right);\quad a_2=a\left[1-\left(\frac{\delta}{H}\right)\right];\quad a=\frac{H}{L};$$
$$Re_1=\frac{\rho_1u_{1avg}\delta}{\mu_1};\quad Re_2=\frac{\rho_2u_{2avg}(H-\delta)}{\mu_2}\qquad (5a\text{-}e)$$

Note that the axial diffusion terms in Eqs. (2) and (3) are negligible as $a_{1,2}<a\ll 1$ The boundary conditions of Eqs. (2) and (3) are given by:

$$\overline{x}=0:\quad \frac{\partial\overline{u}_{1,2}}{\partial\overline{x}}=0,\quad \theta_{1,2}=0\qquad (6a\text{-}d)$$

$$\overline{y}_1=0:\quad \overline{u}_1=0,\quad \frac{\partial\theta_1}{\partial\overline{y}_1}=-1\qquad (6e,6f)$$

$$\overline{y}_1=1,\quad \overline{y}_2=0:\quad \overline{u}_1=\left(\frac{u_{2avg}}{u_{1avg}}\right)\overline{u}_2,\quad \left(\frac{\delta/H}{1-\delta/H}\right)\theta_1=\left(\frac{k_1}{k_2}\right)\theta_2\qquad (6g,6h)$$

$$\overline{y}_1=1,\quad \overline{y}_2=0:\quad \left(\frac{u_{1avg}}{u_{2avg}}\right)\frac{\partial\overline{u}_1}{\partial\overline{y}_1}=\left(\frac{\delta/H}{1-\delta/H}\right)\frac{\partial\overline{u}_2}{\partial\overline{y}_2},\quad \frac{\partial\theta_1}{\partial\overline{y}_1}=\frac{\partial\theta_2}{\partial\overline{y}_2}\qquad (6i,6j)$$

$$\overline{y}_2=1:\quad \overline{u}_2=0,\quad \frac{\partial\theta_2}{\partial\overline{y}_2}=0\qquad (6k,6l)$$

Eq. 6(a,b) require that both co-flows are hydrodynamically fully developed inside the minichannel. Eqs. 6(e, k) necessitate that no slip condition is imposed on both boundaries of the minichannel. Eqs. 6(g, h) require that both velocity and temperature are continuous at the interface and Eqs. 6(i, j) require that both shear stress and heat flux are continuous at the interface between the two streams.

The solution of Eqs. (1) and (2) subjected to the relevant boundary conditions are given by:

$$\overline{u}_1(\overline{y}_1)=\frac{6\overline{y}_1\left[(\delta/H)^2(\mu_2/\mu_1-1)(\overline{y}_1-1)+(\delta/H)\overline{y}_1-1\right]}{2(\delta/H)-3-(\delta/H)^2(\mu_2/\mu_1-1)}\qquad (7)$$

$$\overline{u}_2(\overline{y}_2)=\frac{6(\overline{y}_2-1)[(\delta/H)(\mu_2/\mu_1-1)([1-\delta/H]\overline{y}_2+1)+[1-\delta/H]\overline{y}_2+(\delta/H)]}{(\delta/H)[\delta/H-4](\mu_2/\mu_1-1)-2(\delta/H)-1}\qquad (8)$$

$$\overline{v}_1=\overline{v}_2=0\qquad (9a,9b)$$

Eqs. (7) and (8) are derived based on the fact that $\int_0^1\overline{u}_{1,2}d\overline{y}_{1,2}=1$. The latter integrals reveal the following expressions for $u_{1avg}$ and $u_{2avg}$:

$$\frac{u_{1avg}}{u_r}=\left(\frac{\delta}{H}\right)\left\{\frac{3-2(\delta/H)+(\delta/H)^2(\mu_2/\mu_1-1)}{1+(\delta/H)(\mu_2/\mu_1-1)}\right\}\qquad (10)$$

$$\frac{u_{2avg}}{u_r}=\left(\frac{\mu_1}{\mu_2}\right)\left(1-\frac{\delta}{H}\right)\left\{\frac{1+2(\delta/H)-(\delta/H)(\delta/H-4)(\mu_2/\mu_1-1)}{1+(\delta/H)(\mu_2/\mu_1-1)}\right\}\qquad (11)$$

where $u_r$ is the reference mean primary fluid velocity. When $\delta=H$, $u_{1avg}=u_r=(p_i-p_o)H^2/(12\mu_1L)$. The mass flow rates of both fluids can be obtained using Eqs. (7)-(11):

$$\frac{\dot{m}_1}{\dot{m}_r}=\left(\frac{\delta}{H}\right)^2\left\{\frac{3-2(\delta/H)+(\delta/H)^2(\mu_2/\mu_1-1)}{1+(\delta/H)(\mu_2/\mu_1-1)}\right\}\qquad (12)$$

$$\frac{\dot{m}_2}{\dot{m}_r}=\left(\frac{\rho_2}{\rho_1}\right)\left(\frac{\mu_1}{\mu_2}\right)\left(\frac{\delta}{H}-1\right)^2\left\{\frac{1+2(\delta/H)-(\delta/H)(\delta/H-4)(\mu_2/\mu_1-1)}{1+(\delta/H)(\mu_2/\mu_1-1)}\right\}\qquad (13)$$

where $\dot{m}_r$ is the mass flow rate of the primary fluid when $\delta=H$, $\dot{m}_r=\rho_1(p_i-p_o)H^3/(12\mu_1L)$. The ideal total pumping power requirement for both fluids $P_t$ defined as $P_t=\sum_{l=1}^{2}\dot{m}_l(p_i-p_o)/\rho_l$ can be calculated as:

$$\frac{P_t}{P_r}=\left(\frac{\dot{m}_1}{\dot{m}_o}\right)+\left(\frac{\rho_1}{\rho_2}\right)\left(\frac{\dot{m}_2}{\dot{m}_o}\right)\qquad (14)$$

where $P_r$ is the reference ideal pumping power of the primary fluid; when $\delta=H$, $P_t=P_r=\dot{m}_r(p_i-p_o)/\rho_1$. Let $C$ be $C=\dot{m}c_p$, hence the ratio of $C_1$ to $C_1+C_2$ denoted by $C_R$ is equal to:

$$C_R\equiv\frac{C_1}{C_1+C_2}=[1+C_2/C_1]^{-1}$$
$$=\left[1+\frac{(\delta/H-1)^2\{1+2(\delta/H)-(\delta/H)(\delta/H-4)(\mu_2/\mu_1-1)\}}{(c_{p1}/c_{p2})(\rho_1/\rho_2)(\mu_2/\mu_1)(\delta/H)^2\left\{3-2(\delta/H)+(\delta/H)^2(\mu_2/\mu_1-1)\right\}}\right]^{-1}\qquad (15)$$

The ratio of $C_t=C_1+C_2$ to that of the reference case $(C_r=\dot{m}_rc_{p1})$ represents a comparison between the total thermal capacity of the combined fluids flow and that for the reference case. This ratio is equal to:

$$\frac{C_t}{C_r}=\left(\frac{\dot{m}_1}{\dot{m}_r}\right)+\left(\frac{c_{p2}}{c_{p1}}\right)\left(\frac{\dot{m}_2}{\dot{m}_r}\right)\qquad (16)$$

The Nusselt number between the primary fluid flow and the heated boundary is defined as:

$$Nu_1\equiv\frac{h_1\delta}{k_1}=\frac{1}{\theta_{1W}-\theta_{1m}}\qquad (17)$$

where $h_1$, $\theta_{1m}$ and $\theta_{1W}$ are the convection heat transfer coefficient between the heated boundary and the primary fluid flow $(h_1=q_s''/[T_W-T_{1m}])$, dimensionless mean bulk temperature of the primary fluid and the dimensionless lower boundary temperature $(\theta_{1W}=\theta_1(\overline{x},\overline{y}_1=0))$, respectively. $T_W$ and $T_{1m}$ are the temperature at the heated boundary and the mean bulk temperature of the primary fluid, respectively. The dimensionless mean bulk temperatures of the primary and secondary fluids $\theta_{1m}$ and $\theta_{2m}$ can be computed from the following equations:

$$\theta_{1m}(\overline{x})\equiv\frac{T_{1m}(x)-T_i}{q_s''\delta/k_1}=\int_0^1\overline{u}_1\theta_1d\overline{y}_1\qquad (18)$$

$$\theta_{2m}(\overline{x})\equiv\frac{T_{2m}(x)-T_i}{q_s''(H-\delta)/k_2}=\int_0^1\overline{u}_2\theta_2d\overline{y}_2\qquad (19)$$

The Nusselt number between the interface and the secondary flow is:

$$Nu_2 \equiv \frac{h_2(H-\delta)}{k_2} = \left\{\frac{-1}{\theta_{2I}-\theta_{2m}}\right\}\left(\left.\frac{\partial\theta_2}{\partial\overline{y}_2}\right|_{\overline{y}_2=0}\right) \tag{20}$$

where $h_2$ is the convection heat transfer coefficient between the interface and the secondary fluid flow, $h_2 = q_I''/(T_I - T_{2m})$, $\theta_{2I}$ dimensionless interface temperature $\theta_{2I} = \theta_2(\overline{x}, \overline{y}_2 = 0)$ and $q_I''$ is the heat flux at the interface, $q_I'' = -k_2(\partial T_2/\partial y_2|_{y_2=0})$.

*2.1.1. Integral energy equation of combined fluid flows*

The integral form of the combined energy equation is formed from Eqs. 3(a, b) and can be expressed in the following form:

$$a\left\{Re_1Pr_1\left(\frac{\delta}{H}\right)\frac{d\theta_{1,m}}{d\overline{x}} + Re_2Pr_2\left(1-\frac{\delta}{H}\right)\frac{d\theta_{2,m}}{d\overline{x}}\right\} = 1 \tag{21}$$

*2.1.2. Thermal performance factors*

Let the heat transfer enhancement indicator $\lambda$ be defined as ratio of the lower boundary excess temperature at the exit section for the reference case ($\delta = H$) to that quantity when $\delta < H$. Mathematically, it is equal to:

$$\lambda \equiv \frac{[T_W(x=L)-T_i]|_{\delta=H}}{[T_W(x=L)-T_i]} = \frac{\theta_{1,W}(\overline{x}=1)|_{\delta=H}}{\theta_{1,W}(\overline{x}=1)[\delta/H]} \tag{22}$$

Let the second thermal performance indicator $\gamma$ be defined as ratio of $h_1$ at the exit for the present case to that quantity for the reference case when $\delta = H$. Mathematically, it is equal to:

$$\gamma \equiv \frac{h(x=L)}{h(x=L)|_{\delta=H}} = \left[\frac{Nu(\overline{x}=1)}{Nu(\overline{x}=1)|_{\delta=H}}\right]\left[\frac{1}{(\delta/H)}\right] \tag{23}$$

*2.2. Analytical solution for fully developed condition when $k_2/k_1 \to 0$*

When $k_2/k_1 \to 0$, the interface thermal condition becomes an adiabatic condition. As such, the solution of Eq. 3(a) can be reduced to the following:

$$\theta_1(\overline{x},\overline{y}_1) = \frac{(\delta/H)^2([\mu_2/\mu_1]-1)(\overline{y}_1^4/2-\overline{y}_1^3)+(\delta/H)(\overline{y}_1^4/2)-\overline{y}^3}{2(\delta/H)-3-(\delta/H)^2([\mu_2/\mu_1]-1)} - \overline{y}_1 + \theta_{1,W}(\overline{x}) \tag{24}$$

Eq. (24) was obtained based on the fact that $d\theta_1/d\overline{x} = d\theta_{1,m}/d\overline{x} = d\theta_W/d\overline{x} = 1/(aRe_1Pr_1[\delta/H])$ when $k_2/k_1 \to 0$. As such, $\theta_{1,W}$, $Nu_{1,fd}$ for this case denoted by $(\theta_{1W,fd})_{k_2=0}$ and $(Nu_{1,fd})_{k_2=0}$, respectively, can be obtained which can be arranged into the following forms:

$$(\theta_{W,fd})_{k_2=0} = \frac{\overline{x}}{(\delta/H)(\dot{m}_1/\dot{m}_r)(aRe_rPr_1)} + \frac{1}{(Nu_{1,fd})_{k_2=0}} \tag{25}$$

$$(Nu_{1,fd})_{k_2=0} = \frac{35[-D+2(\delta/H)-3]^2}{13D[D-5(\delta/H)+7]+90(\delta/H)^2-245(\delta/H)+168} \tag{26}$$

where $D = (\delta/H)^2(\mu_2/\mu_1 - 1)$. $(Nu_{1,fd})_{k_2=0}$ reduces to the following when $\mu_2/\mu_1 \to 0$:

$$(Nu_{1,fd})_{k_2=0} = \frac{35([\delta/H]+3)}{([\delta/H]-1)(13[\delta/H]^2+91[\delta/H]+168)} \tag{27}$$

The performance indicators $\lambda$ and $\gamma$ for this case denoted by $(\lambda_{fd})_{k_2=0}$ and $(\gamma_{fd})_{k_2=0}$, respectively, are equal to:

$$(\lambda_{fd})_{k_2=0} = \frac{1+(13/35)(aPe_r)}{(\dot{m}_r/\dot{m}_1)+(\delta/H)(aPe_r)/(Nu_{1,fd})_{k_2=0}} \tag{28}$$

$$(\gamma_{fd})_{k_2=0} = \frac{[-D+2(\delta/H)-3]^2(\delta/H)^{-1}}{D[D-5(\delta/H)+7]+90(\delta/H)^2-245(\delta/H)+168} \tag{29}$$

$(\lambda_{fd})_{k_2=0}$ approaches to $(\lambda_{fd})_{k_2=0,0}$ when $aPe_r$ approaches to zero. Note that $Pe_r = Re_rPr_1$. $(\lambda_{fd})_{k_2=0,0}$ is given by:

$$(\lambda_{fd})_{k_2=0,0} = \frac{\dot{m}_1}{\dot{m}_r} \tag{30}$$

The values of $\delta/H$ that makes $(\lambda_{fd})_{k_2=0,0} > 1$ are those lying between $(\delta/H)_a < \delta/H < 1$. $(\delta/H)_a$ is obtained by solving $\dot{m}_1/\dot{m}_r = 1$. $(\delta/H)_a$ can be correlated to $\mu_2/\mu_1$ by the following equation:

$$(\delta/H)_a = 0.2456(\mu_2/\mu_1)^3 - 0.05119(\mu_2/\mu_1)^2 + 0.2713(\mu_2/\mu_1) + 0.5321 \tag{31}$$

with maximum deviation less than 0.3%. The values of $\delta/H$ that makes $(\gamma_{fd})_{k_2=0} > 1$ are those lying between $0 < \delta/H < (\delta/H)_b$. $(\delta/H)_b$ is obtained by solving $(\gamma_{fd})_{k_2=0} = 1$. A correlation between $(\delta/H)_b$ and $\mu_2/\mu_1$ can be:

$$(\delta/H)_b = 0.1034(\mu_2/\mu_1)^3 - 0.01166(\mu_2/\mu_1)^2 + 0.1567(\mu_2/\mu_1) + 0.7506 \tag{32}$$

with maximum deviation less than 0.21% and $\mu_2/\mu_1 < 1$.

*2.3. Analytical solution for limiting case when $\mu_1/\mu_2 \to 0$ and $c_{p1}/c_{p2} \to 0$*

When $\mu_1/\mu_2 \to 0$ and $c_{p1}/c_{p2} \to 0$, Eq. 3(a) and its boundary conditions reduce to:

$$aPe_o\left(\frac{\delta}{H}\right)^2\frac{\partial\theta_1}{\partial\overline{x}} = \frac{\partial^2\theta_1}{\partial\overline{y}_1^2} \tag{33}$$

$$\overline{x}=0: \quad \theta_1 = 0 \tag{34a}$$

$$\overline{y}_1=0: \quad \frac{\partial\theta_1}{\partial\overline{y}_1} = -1 \tag{34b}$$

$$\overline{y}_1=1: \quad \theta_1 = 0 \tag{34c}$$

Eq. (33) is solvable by the method of separation of variables [29]. It can be shown that the dimensionless primary fluid temperature is equal to:

$$\theta_1(\overline{x},\overline{y}_1) = 1 - \left(\frac{8}{\pi^2}\right)\sum_{n=1}^{\infty}\left\{\frac{\cos([2n-1]\pi\overline{y}_1/2)}{(2n-1)^2}\exp\left(-\frac{[2n-1]^2\pi^2\overline{x}}{4aPe_r[\delta/H]^2}\right)\right\} \tag{35}$$

For the reference case when $\delta = H$, Eq. 3(a) can be solved numerically by well-established methods [30]. When $\delta = H$, $\theta_{1,W}(\overline{x}=1)$ can be correlated to $aPe_r$ by the following equation:

$$\theta_{1,W}(\overline{x}=1,\delta=H) = \frac{-755.65-330.44[aPe_o]-0.074114[aPe_o]^2+0.030555[aPe_o]^3}{1-769.55[aPe_o]-20.317[aPe_o]^2+0.25894[aPe_o]^3} \tag{36}$$

with maximum deviation less than 0.75%. By substituting Eqs. (35) and (36) in Eq. (22), the resulting value of $\lambda$ will be the upper limit value that can be reached ($\lambda_{lim}$) using two immiscible fluids co-flows for a given values of $aPe_r$ and $\delta/H$.

## 3. Numerical methodology and results

Eqs. 3(a, b) are coupled via the interface conditions given by boundary conditions, Eqs. 6(h, j). These equations can be solved without iteration if Eqs. 3(a, b) and 6(h, j) are solved using the

implicit finite-difference method discussed by Blottner [31]. To do so, the previous equations were discretized using two-points backward differencing quotient for the first derivative with respect to $\bar{x}$-direction and three-points central differencing quotients for the first and second derivatives with respect to $\bar{y}_1$ and $\bar{y}_2$ directions. The finite difference equations of Eqs. 3(a, b) and the corresponding equation combining Eqs. 6(h, j) are given by:

$$a_1 Pe_1(\bar{u}_1)_{i,j}\left\{\frac{(\theta_1)_{ij}-(\theta_1)_{i-1,j}}{\Delta\bar{x}}\right\}=\left\{\frac{(\theta_1)_{i,j-1}-2(\theta_1)_{ij}+(\theta_1)_{i,j+1}}{\Delta y_1^2}\right\} \tag{37}$$

$$a_2 Pe_2(\bar{u}_2)_{i,l}\left\{\frac{(\theta_2)_{i,l}-(\theta_2)_{i-1,l}}{\Delta\bar{x}}\right\}=\left\{\frac{(\theta_2)_{i,l-1}-2(\theta_2)_{i,l}+(\theta_2)_{i,l+1}}{\Delta y_2^2}\right\} \tag{38}$$

$$-\left(\frac{\Delta\bar{y}_2}{\Delta\bar{y}_1}\right)(\theta_1)_{i,j=n_1-1}+\left[\left(\frac{\Delta\bar{y}_2}{\Delta\bar{y}_1}\right)\left(\frac{1-\delta/H}{\delta/H}\right)\left(\frac{k_1}{k_2}\right)+1\right](\theta_2)_{i,l=1}-(\theta_2)_{i,l=2}=0 \tag{39}$$

where $Pe_{1,2} = Re_{1,2}Pr_{1,2}$. The pair $(i,j)$ represents the location of the discretized point in the numerical grid of the primary fluid domain. The pair $(i,l)$ is the location of the discretized point in the numerical grid of the secondary fluid domain.

The resulting $n_1 + n_2 - 1$ $(n_1 = 201, n_2 = 201)$ tri-diagonal systems of algebraic equations obtained by Eqs. (37)-(39) at a given $i$–section were solved using the well-established Thomas algorithm discussed by Blottner [30]. The numbers $n_1$ and $n_2$ represent the total number of nodes along each $j$-line and $l$-line, respectively. The interface is located in the numerical grid at $(i, j = n_1)$ or $(i, l = 1)$. The same procedure was repeated for the consecutive $i$-values until $i$ reached the value $m$ $(m = 501)$ at which $\bar{x} = 1$. Numerical investigations were performed using different mesh sizes to assess and ascertain grid-size independent results. Further, doubling the values of $m$ and $(n_1, n_2)$ results in less than 0.4% error in the calculated parameters for a moderate $aPe_r$ value.

The numerical method results shown in Fig. 2 and Figs. 7–11 were generated for three different fluids combination cases. The data for three different cases are shown in Table 1. All cases have $k_2/k_1 < 1.0$ and $\rho_2/\rho_1 < 1.0$. This is to assure that the primary fluid residues on the heated boundary and it conducts thermal energy from it maximally. $c_{p2}/c_{p1}$ for case II is larger than one while that of cases I and III are smaller than one. $\mu_2/\mu_1$ for case I is larger than one while that of cases II and III are smaller than one. The numerical results of case III were compared with the analytical solution given by Eq. (26) as can be shown in Fig. 2. The numerical results match well with the analytical solution when $\delta/H > 0.2$ and $aPe_o \leqslant 0.6$ as these conditions best satisfy the constraints of Eq. (26).

## 4. Discussion of the results

### 4.1. Hydrodynamic performance of the two immiscible co-flows

Fig. 3 shows the fully developed velocity profiles for the different cases. It is noticed that the primary fluid flow is aided by the secondary fluid flow for cases II and III where $\mu_2/\mu_1 < 1.0$. However, it is retarded by the secondary fluid flow for case I where $\mu_2/\mu_1 > 1.0$. It is noticed from Fig. 4 that the total pumping power for both flows is smaller than that for the reference case where the primary fluid flow occupies the total minichannel height when $\mu_2/\mu_1 > 1.0$. This is expected as an increase in $\mu_2$ causes a reduction in $u_{2avg}$ resulting in a reduction in the secondary flow rate. It is observed from Fig. 5 that the mass flow rate of the primary fluid can be larger than that for the reference case. This phenomenon occurs when $\mu_2/\mu_1 < 1.0$ and $(\delta/H)_a < \delta/H < 1.0$. This indicates that larger heat transfer rate can be attainable when the coolant is partially filling the minichannel.

### 4.2. Thermal capacities assessment of the two immiscible fluids co-flows

Fig. 6 shows that the primary to secondary flows relative thermal capacities ratio ($C_R$) increases as both $\mu_2/\mu_1$ and $\delta/H$ increase. This is because both effects decrease the secondary fluid flow rate. Furthermore, a decrease in $(\rho c_p)_2$ causes a decrease in the secondary flow thermal capacity. Thus, $C_R$ increases as $(\rho c_p)_2/(\rho c_p)_1$ decreases as shown Fig. 6. Notice that when $C_R$ decreases much below $C_R = 0.95$, the interfacial heat flux increases for case III. Thus, the deviation between the numerical results and Eq. (26) becomes more apparent as displayed in Fig. 2. It is shown in Fig. 6 that the dimensionless total system thermal capacity $C_t/C_o$ is much larger than one when both $\mu_1/\mu_2$ and $(\rho c_p)_2/(\rho c_p)_1$ are much larger than one, and as $\delta/H$ decreases. This indicates that the combined flow

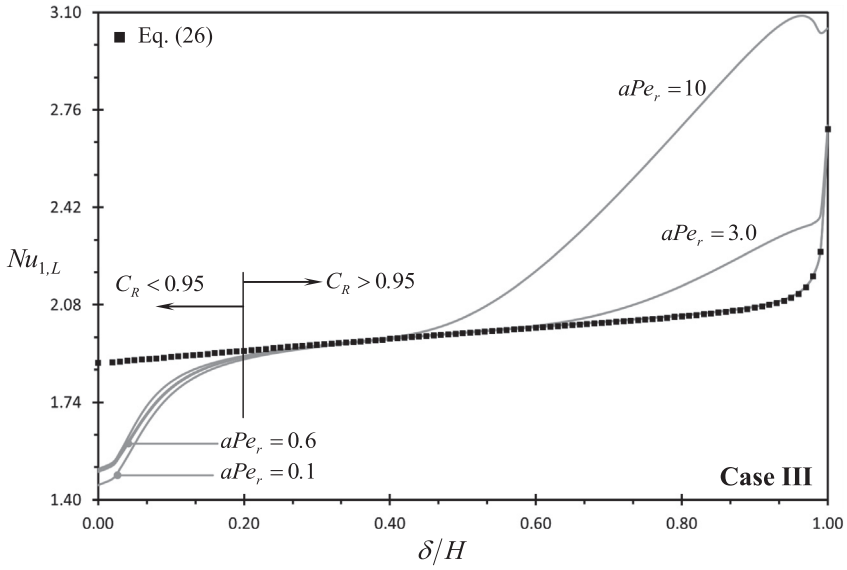


**Fig. 2.** Effects of $\delta/H$ and $aPe_r$ on $Nu_{1,L}$ for case III ($a = 0.1$, $c_{p2}/c_{p1} = 0.241$, $k_2/k_1 = 0.0429$, $\mu_2/\mu_1 = 0.02164$, $\rho_2/\rho_1 = 1.165 \times 10^{-3}$, $Pr_1 = 5.83$).

**Table 1**
Cases studied for the numerical results.

| Property | Case I | | Case II | | Case III | |
|---|---|---|---|---|---|---|
| | Fluid (1) Water | Fluid (2) Oil | Fluid (1) Mercury | Fluid (2) Water | Fluid (1) Water | Fluid (2) Air |
| Density (kg m$^{-3}$) | 997 | 884 | 13,529 | 997 | 997 | 1.1614 |
| Specific heat (J kg$^{-1}$ K$^{-2}$) | 4179 | 1909 | 139.3 | 4179 | 4179 | 1007 |
| Thermal conductivity (W m$^{-1}$ K$^{-1}$) | 0.613 | 0.145 | 8.54 | 0.613 | 0.613 | 0.0263 |
| Viscosity (N s m$^{-2}$) | $8.55 \times 10^{-4}$ | 0.486 | $1.52 \times 10^{-3}$ | $8.55 \times 10^{-4}$ | $8.55 \times 10^{-4}$ | $1.85 \times 10^{-5}$ |
| Prandtl number | 5.83 | 6398 | 0.0248 | 5.83 | 5.83 | 0.708 |
| $c_{p2}/c_{p1}$ | | 0.4568 | | 30 | | 0.2410 |
| $k_2/k_1$ | | 0.2365 | | 0.07178 | | 0.04290 |
| $\mu_2/\mu_1$ | | 568.4 | | 0.5625 | | 0.02164 |
| $\rho_2/\rho_1$ | | 0.8867 | | 0.07369 | | $1.165 \times 10^{-3}$ |

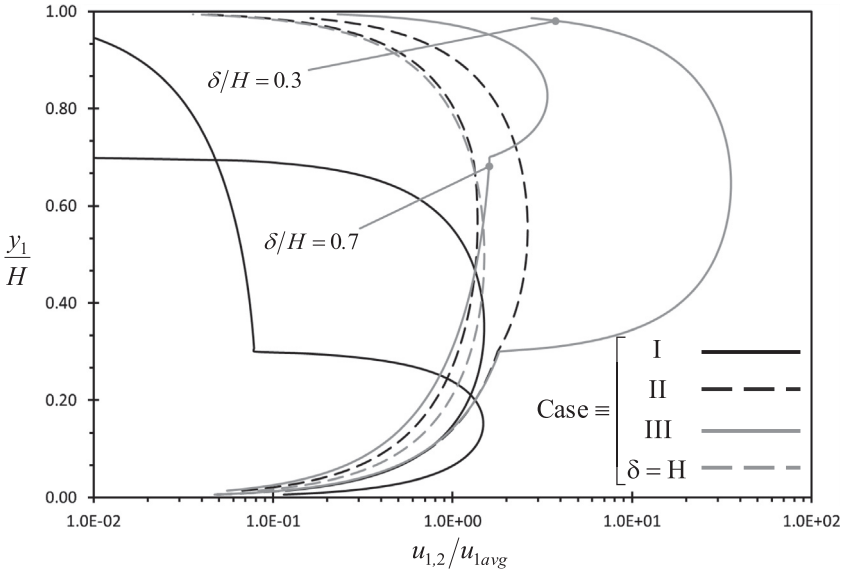


**Fig. 3.** Velocity profile for the three different cases.

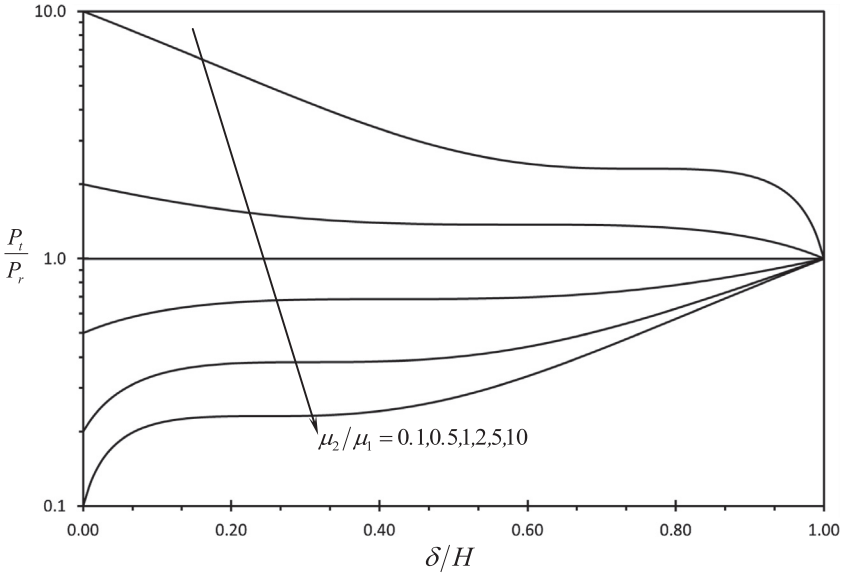


**Fig. 4.** Effects of $\delta/H$ and $\mu_2/\mu_1$ on $P_t/P_r$.

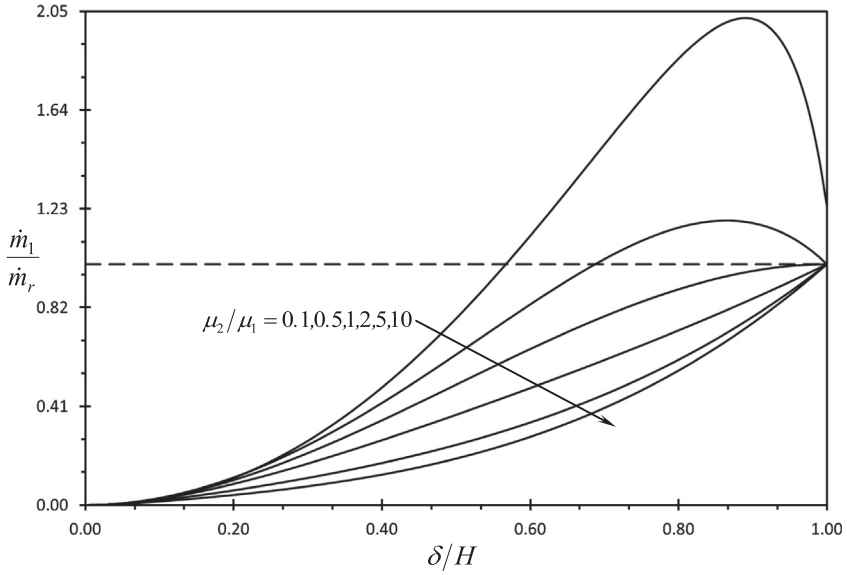


**Fig. 5.** Effects of $\delta/H$ and $\mu_2/\mu_1$ on $\dot{m}_1/\dot{m}_r$.

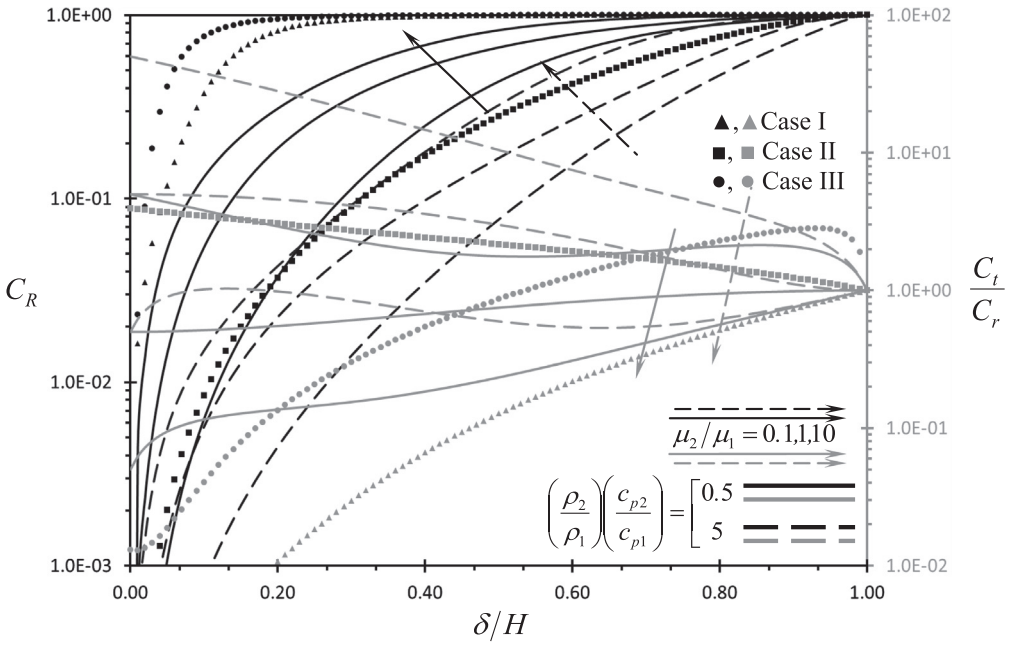


**Fig. 6.** Effects of $\delta/H$ and $\mu_2/\mu_1$ on $C_R$ and $C_t/C_r$.

systems can have larger heat transfer rates than the reference system at the previous conditions.

### 4.3. Thermal performance of the two immiscible co-flows for case I

For case I, $\overline{u}_1$ near the heated boundary is larger than that for the reference case as shown in Fig. 3. This effect produces larger $h_{1,L}$ coefficient as compared to the reference case at smaller $aPe_r$ values. On the other hand, $h_{1,L}$ is expected to decrease as $\delta/H$ decreases at smaller $aPe_r$ as the interfacial heat flux increases and $u_{1avg}$ decreases as $\delta/H$ decreases. Meanwhile, $h_{1,L}$ for both cases increases as $aPe_r$ increases due to an increase in the thermal entry region effect. However, heat transfer to the reference system is more influenced by the thermal entry region than that for the case I as $C_t/C_r < 1$. Due to the previous reasoning, $\gamma$ is expected to be larger than one and have a local maximum value at smaller $\delta/H$ values as shown in Fig. 7. Unfortunately, it is shown in this figure that $\lambda < 1$. The reason behind this finding is that the primary fluid mean temperature at exit, $T_{1m,L}$, for case I is always larger than that for the reference case as $C_t/C_r < 1$. Since the heated boundary temperature at exit is equal to $T_{1W,L} = T_{1m,L} + q''_s/h_{1,L}$, $\lambda$ increases as $aPe_r$ increases as seen in Fig. 7. This is because $T_{1m,L}$ decreases and $h_{1,L}$ increases as $aPe_r$ increases. Another reason for inappropriateness of using the (water–oil) combination is that viscous dissipation in the oil layer is apparent due to its large viscosity. This can further impede the heat transfer inside the microchannel. The difference between the densities of these fluids is relatively small and the oil Prandtl number is very large thus; the two flows can

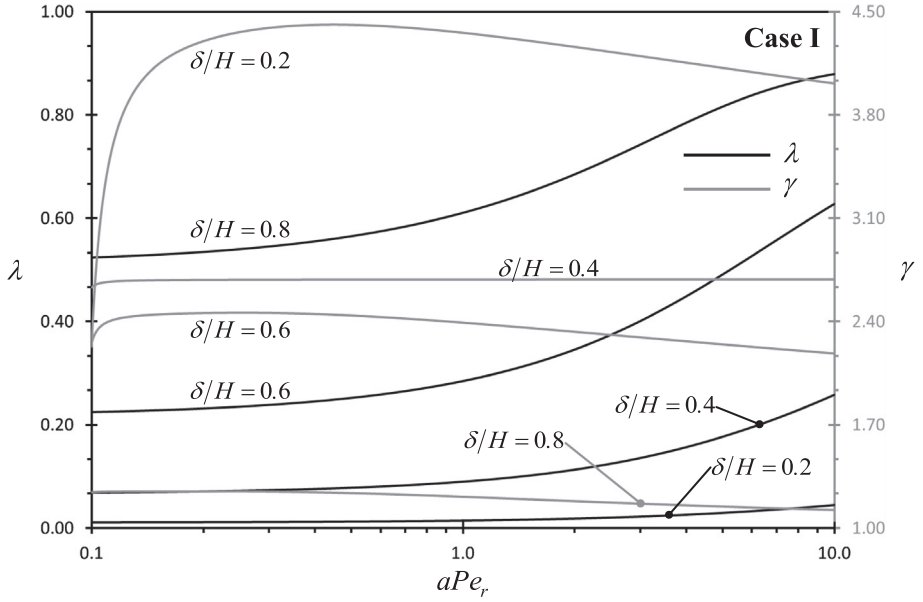


**Fig. 7.** Effects of $aPe_r$ and $\delta/H$ on performance indicators $\lambda$ and $\gamma$ for case I ($a = 0.1,\ c_{p2}/c_{p1} = 0.4568,\ k_2/k_1 = 0.2365,\ \mu_2/\mu_1 = 568.4,\ \rho_2/\rho_1 = 0.8867,\ Pr_1 = 5.83$).

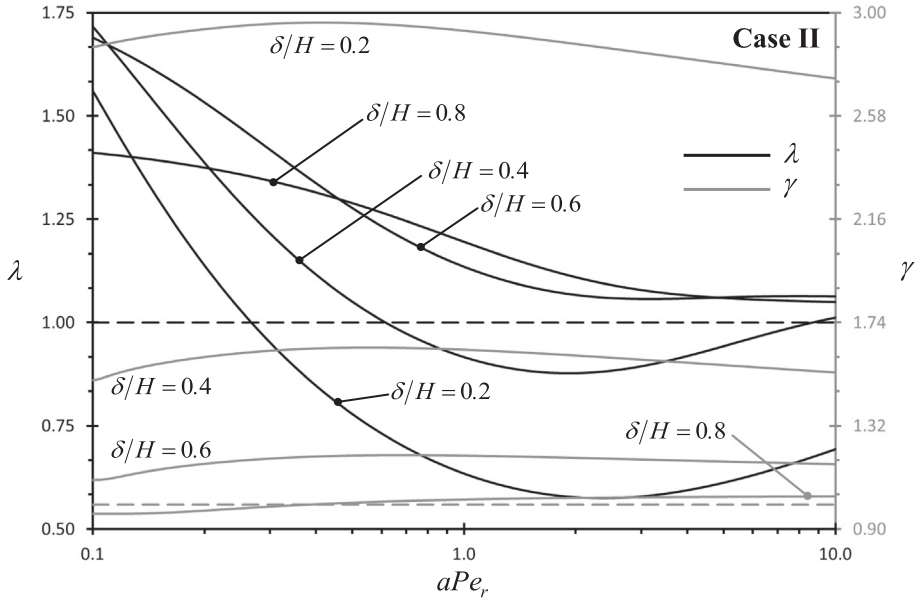


**Fig. 8.** Effects of $aPe_r$ on performance indicators $\lambda$ and $\gamma$ for case II ($a = 0.1,\ c_{p2}/c_{p1} = 30,\ k_2/k_1 = 0.07178,\ \mu_2/\mu_1 = 0.5625,\ \rho_2/\rho_1 = 0.07369,\ Pr_1 = 0.0248$).

hydrodynamically and thermally be unstable even at small Reynolds numbers [32]. However, this combination has no use in our study.

### 4.4. Thermal performance of the two immiscible co-flows for case II

As noticed from Figs. 7 and 8, the values of $\gamma$ for case II are smaller than that for case I. This is because of the following: (1) the system for case II has smaller $\overline{u}_1$ values near the heated boundary as shown in Fig. 3, and (2) the system for case II will have larger interfacial heat flux $q_I''$ as $C_t/C_r > 1$ for case II. Fig. 8 demonstrates that $\lambda$ can be larger than one. At very small $aPe_r$ values, $T_{1W,L}$ approaches $T_{1m,L}$ which is expected to be smaller than that for the reference case as $C_t/C_r > 1$ for case II. As $aPe_r$ increases, $q_I''/q_s''$ for case II becomes smaller than that for the reference case as $k_2/k_1 \ll 1$ for case II. Also, the difference between bulk temperature for the reference case and that for case II decreases. These cause $\lambda$ to decrease as $aPe_r$ increases. Additional increases in $aPe_r$ cause further increases in $h_{1,L}$. This is because the primary flow for case II has wider thermal entry region than that for the reference case as both $C_t/C_r$ and $Pr_2/Pr_1$ are larger than one for case II, $1 < C_t/C_r < 3.93$ and $Pr_2/Pr_1 = 235.1$. Accordingly, $\lambda$ can have a minimum value at specific $aPe_r$ as seen from Fig. 8. In addition, $C_1$ increases as $\delta/H$ increases causing a reduction in $T_{1m,L}$. In contrast, $q_I''$ is expected to significantly be reduced when $\delta$ increases since $k_2/k_1 \ll 1$ for case II. This causes $T_{1m,L}$ to increase as $\delta$ increases after reaching its minimum value. Thus, $\lambda$ will have a local minimum value at specific $\delta/H$ as shown in Fig. 9. Finally, It is worth noting that the (mercury, water) combination has a very large density difference and that the mercury Prandtl number is very small. These dampen any flow instability due to viscosity stratification [32] or due to dissipation.

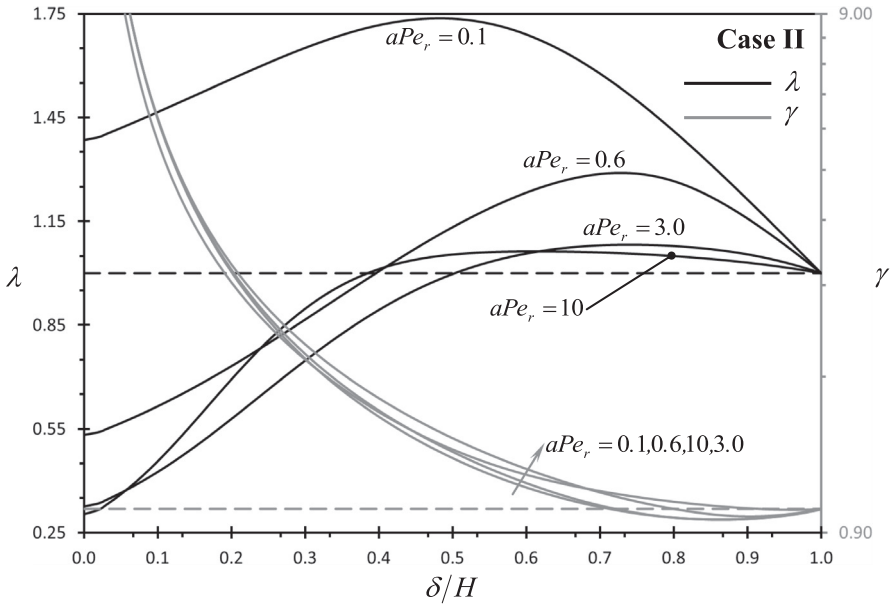


**Fig. 9.** Effects of $\delta/H$ and $aPe_r$ on performance indicators $\lambda$ and $\gamma$ for case II ($a = 0.1,\ c_{p2}/c_{p1} = 30,\ k_2/k_1 = 0.07178,\ \mu_2/\mu_1 = 0.5625,\ \rho_2/\rho_1 = 0.07369,\ Pr_1 = 0.0248$).

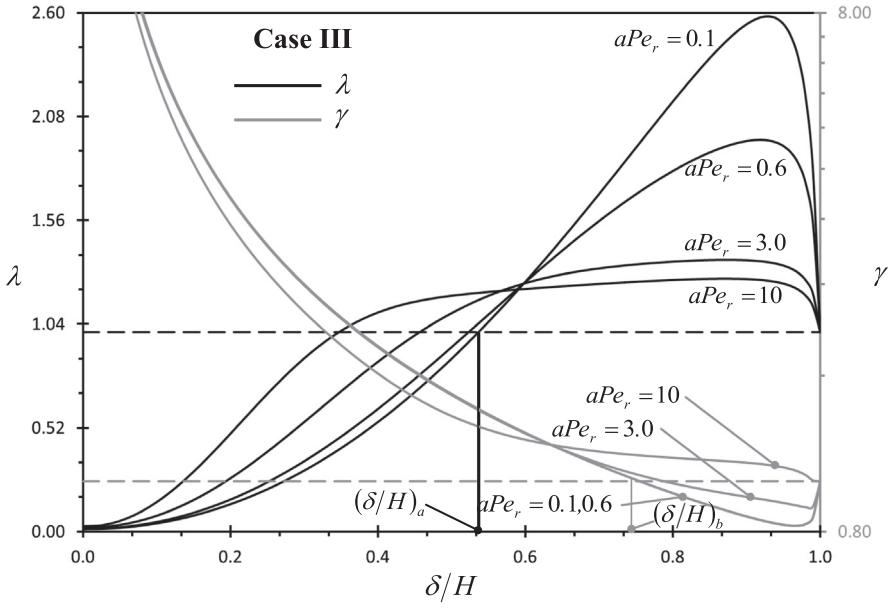


**Fig. 10.** Effects of $\delta/H$ and $aPe_r$ on performance indicators $\lambda$ and $\gamma$ for case III ($a = 0.1,\ c_{p2}/c_{p1} = 0.241,\ k_2/k_1 = 0.0429,\ \mu_2/\mu_1 = 0.02164,\ \rho_2/\rho_1 = 1.165 \times 10^{-3},\ Pr_1 = 5.83$).

### 4.5. Thermal performance of the two immiscible fluids co-flows for case III

The values of $(\delta/H)_a$ and $(\delta/H)_b$ obtained from Eqs. (31) and (32) for case III are equal to $(\delta/H)_a = 0.538$ and $(\delta/H)_b = 0.754$. These values well match those obtained numerically as can be seen in Fig. 10. The latter values are equal to 0.536 and 0.758, respectively. As $aPe_r$ increases when $(\delta/H) < (\delta/H)_a$, the behavior of $\lambda$ as function of $(\delta/H)$ and $aPe_r$ seen in Figs. 10 and 11, respectively, can be attributed to the same controlling factors mentioned earlier. It should be mentioned that the primary flow is expected to have a wider thermal entry region than the reference case when $a_1Pe_1 > aPe_r \rightarrow (\delta/H)(\dot{m}_1/\dot{m}_o) > 1$. The values of $\delta/H$ that satisfy the previous inequality are those lying between $(\delta/H)_c < \delta/H < 1$ where a correlation of $(\delta/H)_c$ can be presented as:

$$(\delta/H)_c = -0.6309(\mu_2/\mu_1)^3 + 0.818(\mu_2/\mu_1)^2 + 0.1659(\mu_2/\mu_1) + 0.6495 \quad (40)$$

with maximum deviation less than 1.6% and $(\mu_2/\mu_1) < 1$. Note that $(\delta/H)_c > (\delta/H)_a$.

### 4.6. Upper thermal performance limit and recommendations

Based on Fig. 12, larger $\lambda_{\lim}$ values are obtainable under the following conditions: (1) $\delta/H$ close to zero when $aPe_r$ is very small,

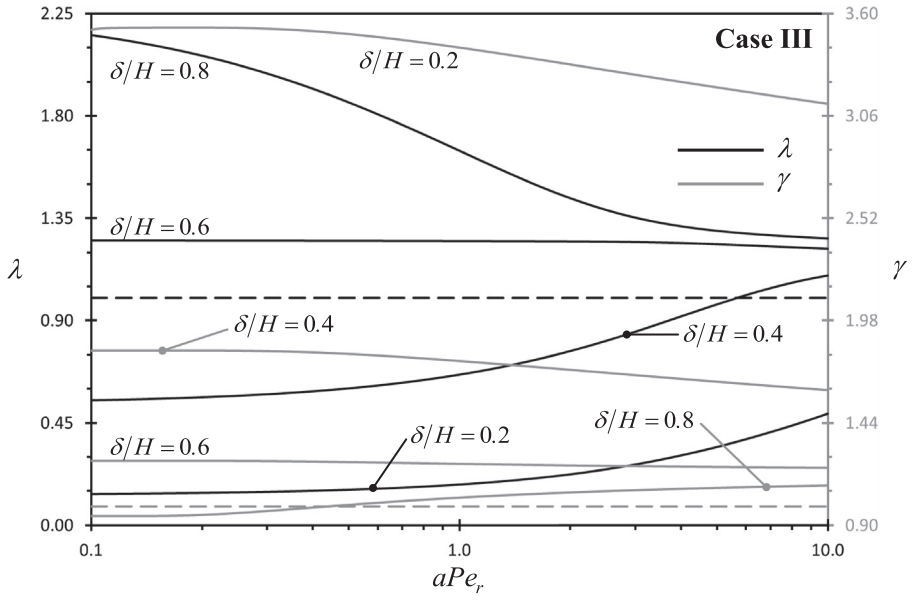


**Fig. 11.** Effects of $aPe_r$ and $\delta/H$ on performance indicators $\lambda$ and $\gamma$ for case III ($a = 0.1,\ c_{p2}/c_{p1} = 0.241,\ k_2/k_1 = 0.0429,\ \mu_2/\mu_1 = 0.02164,\ \rho_2/\rho_1 = 1.165 \times 10^{-3},\ Pr_1 = 5.83$).

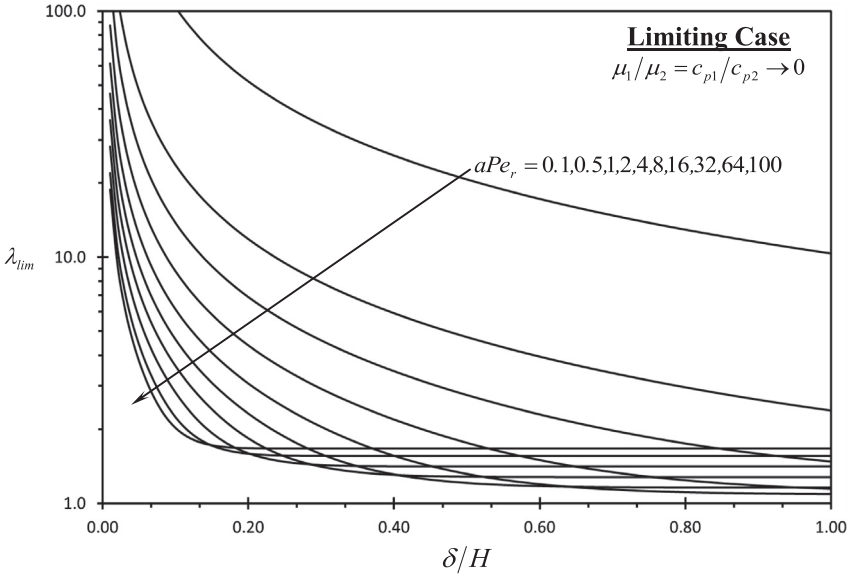


**Fig. 12.** Effects of $\delta/H$ and $aPe_r$ on $\lambda_{\lim}$.

and (2) $\delta/H$ close to one when $aPe_r$ is either very small or very large. From the previous discussions, two different ranges of parameters can be recommended that can result in $\lambda > 1$ when $k_2/k_1 < 1$ and $\rho_2/\rho_1 < 1$:

(a) $(\rho c_p)_2/(\rho c_p)_1 > 1,\quad \mu_2/\mu_1 < 1,\quad (\delta/H) > (\delta/H)_c$ and $k_2/k_1$ closer to one

(b) $(\rho c_p/k)_2/(\rho c_p/k)_1 \gg 1,\quad \mu_2/\mu_1 < 1,\quad aPe_o \ll 1$ and $k_2/k_1$ closer to one.

## 5. Conclusions

Heat transfer enhancement due to co-flowing of two immiscible fluids in a direct contact manner was investigated in this study. Three different fluid combinations were analyzed. These were: (water, oil), (mercury, water) and (water, air). The governing equations for both fluids were solved analytically and numerically. Excellent agreement was obtained between the numerical solution and the analytical solution corresponding to fully developed condition with an adiabatic interface. The enhancement factor was noticed to increase up to a maximum of 2.6 folds for the (water, air) combination when $aPe_r = 0.1$, and up to a maximum of 1.75 folds for the (mercury, water) combination when $aPe_r = 0.1$, while no heat transfer enhancement was obtained for (water, oil) combination. The heat transfer enhancement was achieved because the fluid combination produced an apparent magnification in the primary fluid (coolant) flow rate and a noticeable widening in the thermal entry region resulting in an increase in the interfacial heat flux. The ranges of the fluids relative properties and the flow conditions were identified in this work. This work paves the way for more studies related to heat transfer enhancement by compound mechanisms including co-flowing of two immiscible fluids.

## References


[1] R.J. Goldstein, W.E. Ibele, S.V. Patankar, T.W. Simon, T.H. Kuehn, P.J. Strykowski, K.K. Tamma, J.V.R. Heberlein, J.H. Davidson, J. Bischof, F.A. Kulacki, U. Kortshagen, S. Garrick, V. Srinivasan, Heat transfer—a review of 2003 literature, Int. J. Heat Mass Transfer 49 (2006) (2003) 451–534.

[2] R.J. Goldstein, W.E. Ibele, S.V. Patankar, T.W. Simon, T.H. Kuehn, P.J. Strykowski, K.K. Tamma, J.V.R. Heberlein, J.H. Davidson, J. Bischof, F.A. Kulacki, U. Kortshagen, S. Garrick, V. Srinivasan, K. Ghosh, R. Mittal, Heat transfer—a review of 2004 literature, Int. J. Heat Mass Transfer 53 (2010) 4343–4396.

[3] R.J. Goldstein, W.E. Ibele, S.V. Patankar, T.W. Simon, T.H. Kuehn, P.J. Strykowski, K.K. Tamma, J.V.R. Heberlein, J.H. Davidson, J. Bischof, F.A. Kulacki, U. Kortshagen, S. Garrick, V. Srinivasan, K. Ghosh, R. Mittal, Heat transfer—a review of 2005 literature, Int. J. Heat Mass Transfer 53 (2010) 4397–4447.

[4] K.Y. Kim, J.Y. Choi, Shape optimization of a dimpled channel to enhance turbulent heat transfer, Numer. Heat Transfer A: Appl. 48 (9) (2005) 901–915.

[5] H.M. Metwally, R.M. Manglik, Enhanced heat transfer due to curvature induced lateral vortices in laminar flows in sinusoidal corrugated-plate channels, Int. J. Heat Mass Transfer 47 (10–11) (2004) 2283–2292.

[6] R.A. Stephan, K.A. Thole, Optimization study relevant to louvered fin compact heat exchangers, Int. J. Heat Exch. 6 (1) (2005) 73–92.

[7] Y.P. Cheng et al., Numerical design of efficient slotted fin surface based on the field synergy principle, Numer. Heat Transfer A: Appl. 45 (6) (2004) 517–538.

[8] C.W. Lin, J.Y. Jang, 3D Numerical heat transfer and fluid flow analysis in plate-fin and tube heat exchangers with electrohydrodynamic enhancement, Heat Mass Transfer/Waerme-und Stoffuebertragung 41 (7) (2005) 583–593.

[9] C. Buffone, K. Sefiane, L. Buffone, Heat transfer enhancement in heat pipe applications using surface coating, J. Enhanced Heat Transfer 12 (1) (2005) 21–35.

[10] Y. Yang, Z.G. Zhang, E.A. Grulke, W.B. Anderson, G. Wu, Heat transfer properties of nanoparticle-in-fluid dispersions (nanofluids) in laminar flow, Int. J. Heat Mass Transfer 48 (6) (2005) 1107–1116.

[11] T. Lemenand, C. Durandal, D.D. Valle, H. Peerhossaini, Turbulent direct-contact heat transfer between two immiscible fluids, Int. J. Therm. Sci. 49 (2010) 1886–1898.

[12] A.-R.A. Khaled, K. Vafai, Cooling enhancements inside thin films supported by flexible complex seals in the presence of ultrafine suspensions, J. Heat Transfer – Trans. ASME 125 (2003) 916–925.

[13] A.-R.A. Khaled, K. Vafai, Flow and heat transfer inside thin films supported by soft seals in the presence of internal and external pressure pulsations, Int. J. Heat Mass Transfer 45 (2002) 5107–5115.

[14] A.-R.A. Khaled, K. Vafai, Analysis of flow and heat transfer inside oscillatory squeezed thin films subject to varying clearance, Int. J. Heat Mass Transfer 46 (2006) 631–641.

[15] M. Siddique, A.-R.A. Khaled, N.I. Abdulhafiz, A.Y. Bokhary, Recent advances in heat transfer enhancements: a review report, Int. J. Chem. Eng. 2010 (2010). 106461(1–28).

[16] S. Liu, M. Sakr, A comprehensive review on passive heat transfer enhancements in pipe exchangers, Renew. Sustainable Energy Rev. 19 (2013) 64–81.

[17] A.-R.A. Khaled, Heat transfer analysis through solar and rooted fins, J. Heat Transfer – Trans. ASME 130 (2008) 074503. 1–4.

[18] A.-R.A. Khaled, Heat transfer enhancement through rooted rectangular-and-triangular fins, J. Enhanced Heat Transfer 18 (2011) 127–136.

[19] A.-R.A. Khaled, K. Vafai, Cooling augmentation using microchannels with rotatable separating plates, Int. J. Heat Mass Transfer 54 (2011) 3732–3739.

[20] C. Thianpong, K. Yongsiri, K. Nanan, S. Eiamsa-ard, Thermal performance evaluation of heat exchangers fitted with twisted-ring turbulators, Int. Commun. Heat Mass Transfer 39 (2012) 861–868.

[21] H. Mirzaee, Abdolrahman Dadvand, I. Mirzaee, R. Shabani, Heat transfer enhancement in miicrochannels using an elastic vortex generator, J. Enhanced Heat Transfer 19 (2012) 199–211.

[22] S.-A.B. Al Omari, Enhancement of heat transfer from hot water by co-flowing it with mercury in a mini-channel, Int. Commun. Heat Mass Transfer 38 (2011) 1073–1079.

[23] K. Vafai, N. Zhu, M. Wang, Analysis of asymmetric disk-shaped and flat plate heat pipes, J. Electron. Packag. – Trans. ASME 117 (1995) 209–218.

[24] K. Vafai, N. Zhu, Analysis of a two layered micro-channel heat sink concept in electronic cooling, Int. J. Heat Mass Transfer 42 (1999) 2287–2297.

[25] M.B. Bowers, I. Mudawar, Two-phase electronic cooling using mini-channel and micro-channel heat sink: Part 2 – Flow rate and pressure drop constraint, J. Electron. Packag. – Trans. ASME 116 (1994) 298–305.

[26] F. Durst, Fluid Mechanics: An Introduction to the Theory of Fluid Flows, Springer-Verlag Berlin Heidelberg, Germany, 2008, pp. 388–391.

[27] R.B Bird, W.E Stuart, E.N Lightfoot, Transport Phenomena, Wiley, New York, 1990.

[28] A. Bejan, Convective Heat Transfer, second ed., Wiley, New York, 1995. 32–33.

[29] E. Kreyszig, Advanced Engineering Mathematics, fifth ed., Wiley, New York, 1983.

[30] P.H. Oosthuizen, D. Naylor, Introduction to Convective Heat Transfer Analysis, McGraw-Hill, New York, 1999.

[31] F.G. Blottner, Finite-difference methods of solution of the boundary-layer equations, Am. Inst. Aeronaut. Astronaut. (AIAA) J. 8 (1977) 193–205.

[32] C.-S. Yih, Instability due to viscosity stratification, J. Fluid Mech. 27 (1967) 337–352.